Russian Journal of General Chemistry, Vol. 73, No. 5, 2003, pp. 684–688. Translated from Zhurnal Obshchei Khimii, Vol. 73, No. 5, 2003, pp. 724–728.

Kinetics of Ruddlesden–Popper Phase Formation: III.[1] Mechanism of $Gd_2SrAl_2O_7$ Formation

I. A. Zvereva, V. F. Popova, A. V. Missyul', A. M. Toikka, and V. V. Gusarov

Grebenshchikov Institute of Silicate Chemistry, Russian Academy of Sciences, St. Petersburg, Russia
St. Petersburg State University, St. Petersburg, Russia

Received December 20, 2001

Abstract — Studies on phase formation in the system Gd_2O_3–SrO–Al_2O_3 in the range 900–1530°C showed that the synthesis of $Gd_2SrAl_2O_7$ occur by a mechanism differing from the mechanism of $Ln_2SrAl_2O_7$ formation (Ln = La, Nd, Sm), and the limiting stage is reaction between Gd_2O_3 and $SrAl_2O_4$.

Evidence for the mechanism and kinetics of formation of $Ln_2SrAl_2O_7$ perovskite-like layered compounds (Ln = La, Nd, Sm) have first been obtained in phase-formation studies on Ln_2O_3–SrO–Al_2O_3 systems (Ln = La, Nd, Sm) [1, 2]. Complex aluminates $Ln_2SrAl_2O_7$ crystallizing in the $Sr_3Ti_2O_7$ structural type and belonging to Ruddlesden–Popper phases [3] are formed on a block principle from intergrowing perovskite (P) and rock salt (RS) layers alternating as ...(P)(P)(RS)(P)(P)(RS)... . In the La–Nd–Sm–Gd series, the stability of the P_2/RS-type layered structure increases owing to the transfer from a statistically disordered distribution of Sr^{+2} and Ln^{+3} cations over two nonequivalent sites [$(Ln,Sr)O_{12}$ oxygen cubic octahedra and $(LnSr)O_9$ polyhedra] to their ordered distribution in the $Ln_2SrAl_2O_7$ oxide lattice [4].

Aluminates containing La, Nd, and Sm were found to form, regardless of the starting materials, via formation of $LnAlO_3$ and $LnSrAlO_4$ aluminates having the perovskite P and layered P/RS-type structures, respectively. With all the $Ln_2SrAl_2O_7$ oxides (Ln = La, Nd, Sm), the limiting stage is reaction (1):

$$LnAlO_3 + LnSrAlO_4 \longrightarrow Ln_2SrAl_2O_7. \quad (1)$$

Comparison of the kinetic parameters of $Ln_2SrAl_2O_7$ (Ln = La, Nd, Sm) formation from various reagents and the respective critical temperatures showed that solid-phase reactions in this system are activated only at certain critical temperatures correlating with the temperatures of transition of intergranular formations to a liquid-like state (melting points of two-dimensional nonautonomous phases).

This work presents the results of studies on phase formation in the Gd_2O_3–SrO–Al_2O_3 system at various temperatures and compositions of the starting components.

The kinetics of phase formation in the Gd_2O_3–SrO–Al_2O_3 system were studied by the isothermal annealing–quenching procedure for reactions (2) and (3) in the range 900–1530°C.

$$Gd_2O_3 + Al_2O_3 + SrCO_3 \longrightarrow Gd_2SrAl_2O_7, \quad (2)$$

$$SrAl_2O_4 + Gd_2O_3 \longrightarrow Gd_2SrAl_2O_7. \quad (3)$$

Analysis of the phase composition of the reaction mixture in the Gd_2O_3–SrO–Al_2O_3 system (Table 1) showed that reaction (3) is an intermediate stage of reaction (2). The mechanism of $Gd_2SrAl_2O_7$ formation differs from that of $Ln_2SrAl_2O_7$ oxide formation (Ln = La, Nd, Sm), since $GdAlO_3$ is unstable at the synthesis temperatures [5], and reaction (3) between Gd_2O_3 and the intermediate compound $SrAl_2O_4$ is the limiting process. Changes in the phase composition of the starting mixture during the synthesis of $Gd_2SrAl_2O_7$ by reaction (2) as a function of heat treatment time are illustrated by the X-ray diffraction patterns in Fig. 1.

$Gd_2SrAl_2O_7$ forms much faster than $La_2SrAl_2O_7$ [1] and almost as fast as $Nd_2SrAl_2O_7$ [2]. Thus, in the case of the synthesis of $La_2SrAl_2O_7$, reflexes of $LaAlO_3$ and $LaSrAlO_4$ are predominantly observed after 24-h calcination at 1300°C. The synthesis of $Gd_2SrAl_2O_7$ under the same conditions occurs almost completely, and the X-ray diffraction pattern shows no other reflexes than those of $Gd_2SrAl_2O_7$. The conversions of $Gd_2SrAl_2O_7$ and $Nd_2SrAl_2O_7$ at 1200 and 1300°C are given for comparison in Table 2. The conversions of $Gd_2SrAl_2O_7$ as functions of the

[1] For communication II, see [1].

1070-3632/03/7305-0684 $25.00

Table 1. Phase compositions of the samples resulting from heat treatment of a starting mixture with the chemical composition corresponding to the stoichiometry of $Gd_2SrAl_2O_7$ formed by reactions (2) and (3)

Heat treatment regime		Phase composition of samples after heat treatment	
temperature, °C	time, h	starting components Gd_2O_3, Al_2O_3, $SrCO_3$	starting components Gd_2O_3, $SrAl_2O_4$
900	24–48	Gd_2O_3(cubic), Al_2O_3, SrO ($SrCO_3$)	–
1000	24	Gd_2O_3(cubic), Al_2O_3, SrO ($SrCO_3$)	Gd_2O_3(cubic), $SrAl_2O_4$
	48	Gd_2O_3(cubic), Al_2O_3, SrO ($SrCO_3$), $SrAl_2O_4$, $Gd_2SrAl_2O_7$ (traces)	
1100	24	Gd_2O_3(cubic), $SrAl_2O_4$, $Gd_2SrAl_2O_7$	Gd_2O_3(cubic), $SrAl_2O_4$
	48		Gd_2O_3(cubic), $SrAl_2O_4$, $Gd_2SrAl_2O_7$ (traces)
1200	1–5	Gd_2O_3(cubic), $SrAl_2O_4$, $Gd_2SrAl_2O_7$	Gd_2O_3(cubic), $SrAl_2O_4$, $Gd_2SrAl_2O_7$
	24–48	$Gd_2SrAl_2O_7$, Gd_2O_3(cubic), $SrAl_2O_4$	
1300	1–24	$Gd_2SrAl_2O_7$, Gd_2O_3(cubic), $SrAl_2O_4$	Gd_2O_3(monoclinic), $SrAl_2O_4$, $Gd_2SrAl_2O_7$
	48	$Gd_2SrAl_2O_7$	
1400	1	$Gd_2SrAl_2O_7$, Gd_2O_3, $SrAl_2O_4$ (traces)	$Gd_2SrAl_2O_7$, $SrAl_2O_4$, Gd_2O_3(monoclinic)
	2–48	$Gd_2SrAl_2O_7$	
1500	1–3	$Gd_2SrAl_2O_7$	$Gd_2SrAl_2O_7$, $SrAl_2O_4$, Gd_2O_3(monoclinic)
1530	1–3	$Gd_2SrAl_2O_7$	$Gd_2SrAl_2O_7$, $SrAl_2O_4$, Gd_2O_3(monoclinic)

temperature and time of reaction (2) are given in Fig. 3.

The following two facts attract attention when we compare phase formation in the La–Nd–Sm–Gd series. First, in the Ln_2O_3–SrO–Al_2O_3 systems (Ln = La, Nd, Sm) at 1000°C, $LnAlO_3$ and LnSrAlO4 began to form, whereas in the gadolinium-containing system, $SrAl_2 \cdot O_4$. Second, formation of the $Gd_2SrAl_2O_7$ oxide begins at 1000°C but occurs so slowly that only after 48 h of synthesis only traces of the $Gd_2SrAl_2O_7$ phase appear; at the same time, formation of $La_2SrAl_2O_7$ is activated only at 1300°C, and $Nd_2SrAl_2O_7$ and $Sm_2SrAl_2O_7$ begin to form at 900°C.

The formation of $Gd_2SrAl_2O_7$ by reaction (3) with preliminarily synthesized $SrAl_2O_4$ oxide as a reagent was detected only at 1100°C. We emphasize that

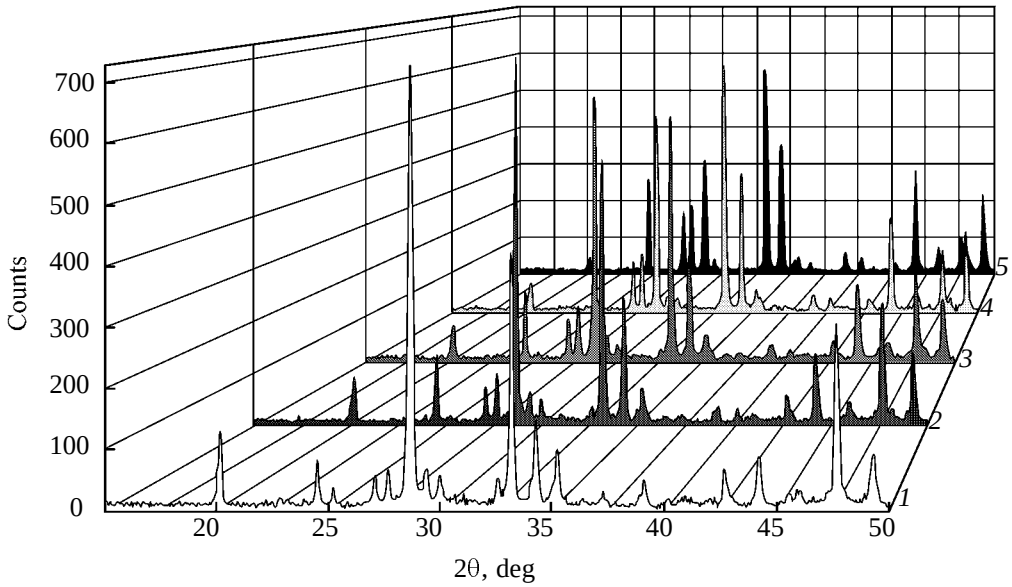

Fig. 1. X-ray diffraction patterns of $Gd_2SrAl_2O_7$ calcined at 1200°C. Calcination time, h: (*1*) 1, (*2*) 3, (*3*) 5, (*4*) 24, and (*5*) 48.

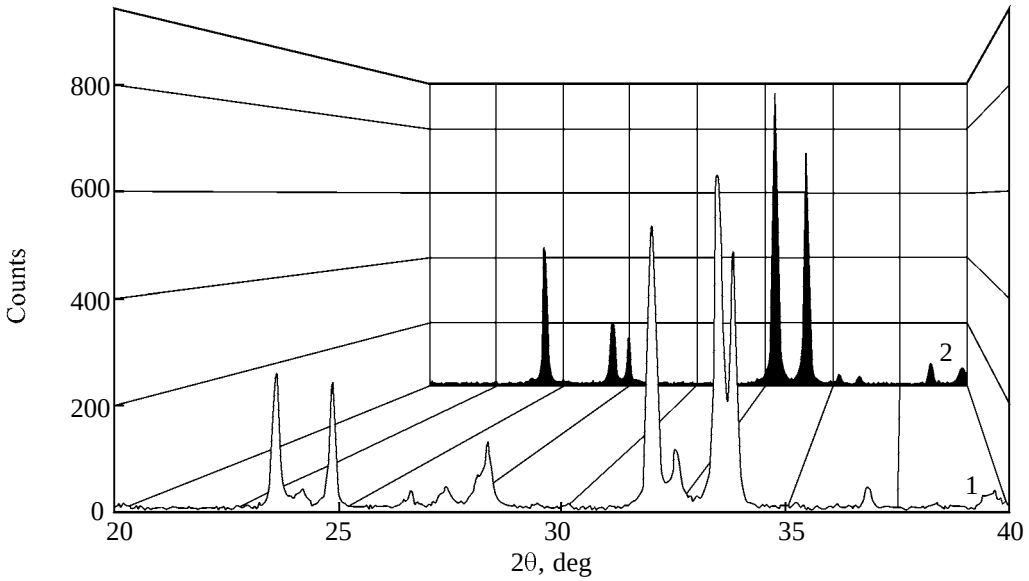

Fig. 2. X-ray diffraction patterns after 24-h calcination at 1300°C. (*1*) $La_2SrAl_2O_7$ and (*2*) $Gd_2SrAl_2O_7$.

Table 2. Conversions of $Gd_2SrAl_2O_7$ and $Nd_2SrAl_2O_7$ at various synthesis times at 1200 and 1300°C

Time, h	1200°C		1300°C	
	$Gd_2SrAl_2O_7$	$Nd_2SrAl_2O_7$	$Gd_2SrAl_2O_7$	$Nd_2SrAl_2O_7$
1	0.62	0.66	0.81	0.80
3	0.71	0.72	0.93	0.90
5	0.75	0.75	0.97	0.97
24	0.85	0.85	1.0	1.0

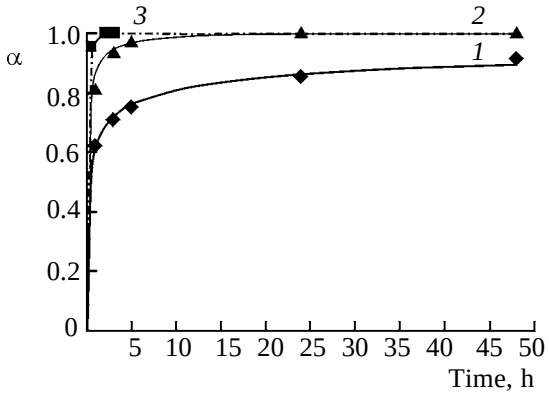

Fig. 3. Kinetics of phase formation in the Gd_2O_3 – $SrCO_3$ – Al_2O_3 mixture (α is the conversion of $Gd_2Sr \cdot Al_2O_7$). Temperature, °C: (*1*) 1200, (*2*) 1300, and (*3*) 1400.

$Ln_2SrAl_2O_7$ is much slower formed when intermediate products, rather than simple oxides, are used as reagents, and this is valid for the entire La–Nd–Sm–Gd series. In the case of $Gd_2SrAl_2O_7$, the reaction is further decelerated by the transition of the Gd_2O_3 oxide from the cubic into monoclinic modification at 1200°C [6]. As a result, the less reactive monoclinic form of Gd_2O_3 appears in the reaction mixture at 1300°C. Note that the synthesis of $Gd_2SrAl_2O_7$ from simple oxides at 1400°C is complete already after 2-h calcination (Table 1). Together the above findings provide evidence to show that the perovskite-like layered oxide $Gd_2SrAl_2O_7$, like $Ln_2SrAl_2O_7$ phases (Ln = La, Nd, Sm), are best synthesized directly from the Gd_2O_3, Al_2O_3, and $SrCO_3$ oxides, even though the mechanism of $Gd_2SrAl_2O_7$ formation in this case is different and involves no formation of the $GdAlO_3$ perovskite phase.

Correlation of the kinetic parameters of $Gd_2Sr \cdot Al_2O_7$ formation and the critical temperatures in the reaction system in study shows that solid-phase reactions in the Gd_2O_3–SrO–Al_2O_3 system are in some sense liquid-phase. This conclusion follows from the fact that chemical reactions in the solid-phase system are activated when two-dimensional nonautonomous phases (intergranular formations) pass into a liquid-like state, thereby sharply increasing the rate of mass transfer in the system.

Thus, in spite of the different mechanisms of formation of $Gd_2SrAl_2O_7$ and $Ln_2SrAl_2O_7$ (Ln = La, Nd, Sm), the reaction rate sharply increases at 1200°C,

i.e. the temperature of the transition of two-dimensional nonautonomous (surface, intergranular) phases on the basis of Al_2O_3 into a liquid-like state [7, 8]. The activation of formation of intermediate products at 900–1000°C, irrespective of their nature and the reaction mechanism, correlates with the temperature of the transition of two-dimensional nonautonomous phases on the basis of $SrCO_3$ into a liquid-like state (750–850°C [7]) and with the phase-transition temperature in strontium carbonate (925°C [9]).

In the electron micrographs of the reaction mixture after 48-h calcination at 1000°C (Fig. 4a) we can see small particles of incipient new phases (intermediate compound $SrAl_2O_4$ and reaction product $Gd_2SrAl_2O_7$) on the background of large particles of unreacted substances. These new phases are located predominantly on the interfaces between large Gd_2O_3, Al_2O_3, and $SrCO_3$ reagent particles, which creates prerequisites for mass transfer, especially upon transition of two-dimensional nonautonomous phases into a liquid-like state. In the micrograph of a singlephase sample of $Gd_2SrAl_2O_7$ after 48-h calcination at 1300°C (Fig. 4b) we can see particles of almost the same size and shape, clearly isolated from each other.

Thus, the structural and chemical transformations in the Gd_2O_3 –SrO–Al_2O_3 system and the kinetics of $Gd_2SrAl_2O_7$ formation reveal one more factor affecting the mechanism of formation of $Ln_2SrAl_2O_7$ perovskite-like layered oxides. This factor is the stability of $LnAlO_3$ oxides crystallizing in the perovskite structural type. As a result, $Gd_2SrAl_2O_7$, unlike $La_2SrAl_2O_7$, $Nd_2SrAl_2O_7$, and $Sm_2SrAl_2O_7$, forms via reaction between $SrAl_2O_4$ and Gd_2O_3.

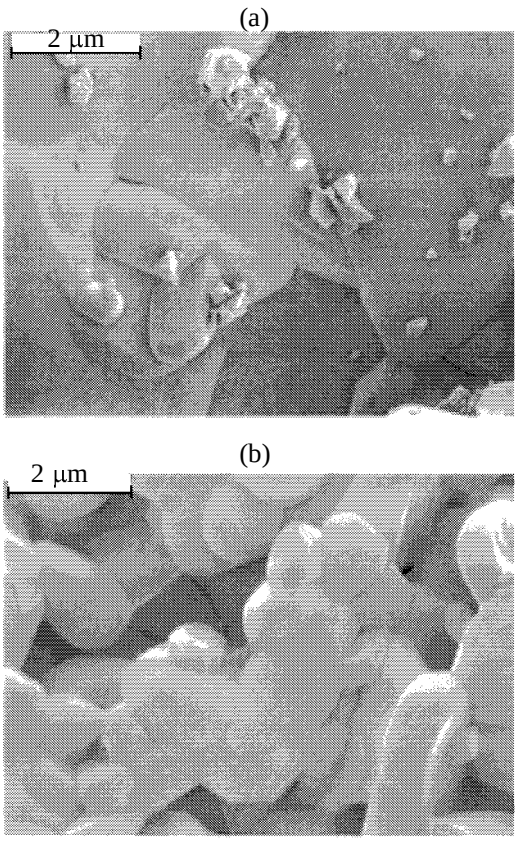

Fig. 4. Electron micrographs of sections of ceramic samples of the reaction mixture corresponding to reaction (2) after 48-h calcination at (a) 1000 and (b) 1300°C.

EXPERIMENTAL

As starting materials we used gadolinium oxide (SST brand, 99.99%), strontium carbonate (7–2 brand, special purity grade, Technical Specifications 6-09-01-659-91), and finely dispersed aluminum oxide (Johnson Matthey 99.99%, 1–15 μm) containing a certain quantity of γ-modification. Reagent mixtures (5 g) with the stoichiometry of $Ln_2SrAl_2O_7$ were prepared by mechanical stirring in a KM-1 agate ball mill for 1.5 h. The samples were pressed into cylinders 15 mm in diameter and 3–4 mm in thickness under a pressure of 500 MPa. The samples were sintered in a furnace with a platinum heater. The isothermal regime of heat treatment was maintained with an accuracy of ±1 K using an RIF-101 precise programmed controller.

Phase composition was controlled by X-ray diffracation. The X-ray diffracion patterns were recorded on a Philips Analytical X-ray PW-3020 diffractometer (CuK_α radication) in the 2θ range 5°–50°. Phase identification was performed using the Diffrac-AT program complex (Version 3.1). Quantitative X-ray phase analysis was performed by the procedure described in [10].

The surface electron micrographs were obtained on a Hitachi-2000 scanning electron microscope.

ACKNOWLEDGMENTS

The work was carried out in the framework of the *Integratsiya* Special Federal Program and financially supported by the Russian Foundation for Basic Research (project no. 00-03-32567).

REFERENCES

1. Zvereva, I.A., Popova, V.F., Pylkina N.S., and Gusarov, V.V., *Zh. Obshch. Khim.*, 2003, vol. 73, no. 1, p. 47.
2. Zvereva, I.A., Popova, V.F., Vagapov, D.A., Toik-

ka, A.M., and Gusarov, V.V., *Zh. Obshch. Khim.*, 2001, vol. 71, no. 8, p. 1254.

3. Ruddlesden, S.N. and Popper, P., *Acta Crystallogr.*, 1958, vol. 11, no. 1, p. 54; Wells, A.F., *Structural Inorganic Chemistry*, Oxford: Oxford Univ. Press, 1986.
4. Zvereva, I.A., Smirnov, Yu.E., Vagapov, D.A., and Choisnet, J., *Zh. Obshch. Khim.*, 2000, vol. 70, no. 12, p. 1957.
5. Bondar', I.A., Shirvinskaya, A.K., Popova, V.F., Mochalov, I.V., and Ivanov, A.O., *Dokl. Akad. Nauk SSSR*, 1979, vol. 246, no. 5, p. 1132.
6. Warshaw, J. and Roy, R., *J. Phys. Chem.*, 1961, vol. 65, no. 11, p. 2048.
7. Gusarov, V.V. and Suvorov, S.A., *Zh. Prikl. Khim.*, 1990, vol. 63, no. 8, p. 1689.
8. Gusarov, V.V., *Thermochim. Acta*, 1995, vol. 256, no. 2, p. 467.
9. Gusarov, V.V., Ishutina, Zh.N., Malkov, A.A., and Malygin, A.A., *Dokl. Ross. Akad. Nauk*, 1997, vol. 357, no. 2, p. 203.
10. *Rukovodstvo po rentgenovskomu issledovaniyu mineralov* (Handbook on X-ray Analyisis of Minerals), Frank-Kamenetskii, V.A., Ed., Leningrad: Nedra, 1975.